

Paper A

Iron-Corrole Complexes | Hot Paper |

Wolves in Sheep's Clothing: μ -Oxo-Diiron Corroles RevisitedSumit Ganguly, Hugo Vazquez-Lima,* and Abhik Ghosh*^[a]

Abstract: For well over 20 years, μ -oxo-diiron corroles, first reported by Vogel and co-workers in the form of μ -oxo-bis[(octaethylcorrolato)iron] (Mössbauer δ 0.02 mm s $^{-1}$, ΔE_Q 2.35 mm s $^{-1}$), have been thought of as comprising a pair antiferromagnetically coupled low-spin Fe IV centers. The remarkable stability of these complexes, which can be handled at room temperature and crystallographically analyzed, present a sharp contrast to the fleeting nature of enzymatic, iron(IV)-oxo intermediates. An array of experimental and theoretical methods have now shown that the iron centers in these complexes are not Fe IV but intermediate-spin Fe III coupled to a corrole $^{2-}$. The intramolecular spin couplings in $\{\text{Fe}[\text{TPC}]\}_2(\mu\text{-O})$ were analyzed via DFT(B3LYP) calculations in terms of the Heisenberg-Dirac-van Vleck spin Hamiltonian $H = J_{\text{Fe-corrole}}(S_{\text{Fe}} \cdot S_{\text{corrole}}) + J_{\text{Fe-Fe}}(S_{\text{Fe}} \cdot S_{\text{Fe}}) + J_{\text{Fe'-corrole}}(S_{\text{Fe'}} \cdot S_{\text{corrole}})$, which yielded $J_{\text{Fe-corrole}} = J_{\text{Fe'-corrole}} = 0.355$ eV (2860 cm $^{-1}$) and $J_{\text{Fe-Fe}} = 0.068$ eV (548 cm $^{-1}$). The unexpected stability of μ -oxo-diiron corroles thus appears to be attributable to charge delocalization via ligand noninnocence.

High-valent iron-oxo intermediates hold iconic status in bioinorganic chemistry on account of their unique, high reactivities.^[1] Thus, the compound I intermediate of cytochrome P450 has long been known for its ability to oxidize a variety hydrocarbons other than methane,^[2] whereas methane monooxygenase Compound Q, which has a bis(μ -oxo)diiron(IV) "diamond core", oxidizes even methane.^[3] A variety of other iron(IV)-oxo intermediates, both enzymatic and synthetic, have been generated and characterized over the last 20 years.^[1] These too are highly reactive, and only a handful of synthetic iron(IV)-oxo species have lent themselves to single-crystal X-ray crystallographic analysis, and that too only at low temperature and with the utmost care.^[4] Against this backdrop, μ -oxo-diiron corroles, of which the first example $\{\text{Fe}[\text{OEC}]\}_2\text{O}$ (OEC = 2,3,7,8,12,13,17,18-octaethylcorrole) was reported by Vogel and co-workers over twenty years ago,^[5] are astonishingly stable,

even allowing manipulations such as column chromatography and storage under ordinary conditions.^[6,7] Based on its Mössbauer (δ 0.02 mm s $^{-1}$, ΔE_Q 2.35 mm s $^{-1}$) and structural characteristics, Vogel and co-workers formulated the compound as a (μ -oxo)diiron(IV) species. Yet it appears that they also harbored a certain unease with this description, as evidenced by the question mark in the background of their 1994 *Angewandte Chemie* cover graphic (Figure 1); wisely, as it turns out. Over the years, however, the Fe IV formulation has never been questioned and indeed has been tacitly assumed in all subsequent studies of μ -oxo-diiron corroles.^[6,7]

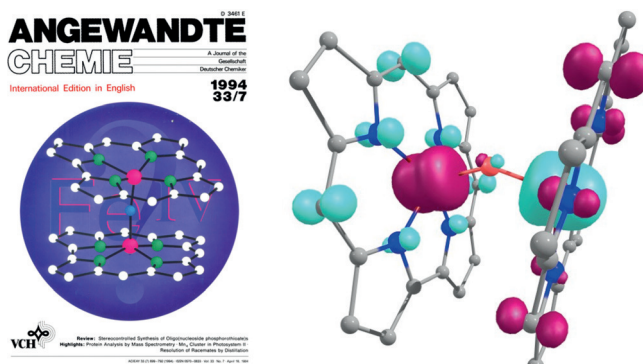


Figure 1. The question mark in the background of Vogel and co-workers' 1994 cover graphic has proved prescient: BS-B3LYP calculations have revealed a complex, intramolecularly spin-coupled electronic structure that may be best described as: corrole $^{2-}$ (↓)-Fe III (↑↑↑)-Fe III (↓↓↓)-corrole $^{2-}$ (↑).

In recent years, many metallocorroles,^[8] including Cu,^[9–11] FeCl,^[12] FeNO,^[13] MnCl,^[14] and some Pt^[15] corroles, have been recognized as noninnocent; that is, the corrole ligand is best viewed as corrole $^{2-}$ as opposed to corrole $^{3-}$. The evidence for such a formulation has originated from a variety of sources, including NMR and EPR spectroscopy, X-ray crystallography, and quantum-chemical calculations, among others. For *meso*-tris(*para*-X-phenyl)corrole (TpXPC) derivatives, electronic absorption spectroscopy has provided a particularly simple, empirical probe. For noninnocent complexes,^[11–17] the Soret maxima undergo significant redshifts with increasing electron-donating character of the *meso*-aryl *para*-substituents. For innocent (that is, corrole $^{3-}$) metallocorroles,^[16–18] on the other hand, the Soret maxima exhibit no such sensitivity to *meso*-aryl substituents. A DFT study of copper triarylcortrooles suggests that the substituent-sensitive Soret feature is an aryl-to-corrole $^{2-}$ LL'CT transition.^[10c] Our early work on μ -oxo-diiron TpXPC derivatives showed that the Soret maximum redshifts modestly across the series X = CF₃ (383 nm) → H (386 nm) → Me (389 nm). We sur-

[a] S. Ganguly, Dr. H. Vazquez-Lima, Prof. Dr. A. Ghosh
Department of Chemistry and Center for Theoretical and Computational Chemistry
UiT – The Arctic University of Norway, 9037 Tromsø (Norway)
E-mail: hugo.vazquez@uit.no
abhik.ghosh@uit.no

Supporting information for this article (selected spectra and DFT optimized coordinates; 10 pages) is available on the WWW under <http://dx.doi.org/10.1002/chem.201601062>.

mised that, although small, these spectral shifts might be indicative of a noninnocent corrole. Accordingly, we synthesized a fourth member of the series, with $X=OMe$, and found it to exhibit a strongly perturbed optical spectrum (Figure 2). Thus, although the Soret maximum (375 nm) turned out to be blue-shifted relative to those of the other three complexes, a prominent shoulder at about 410 nm (Table 1) appeared to be a plausible candidate for the LL'CT transition mentioned above. These results planted the first seeds of suspicion in our minds in regard to a simple Fe^{IV} formulation of μ -oxo-diiron corroles.

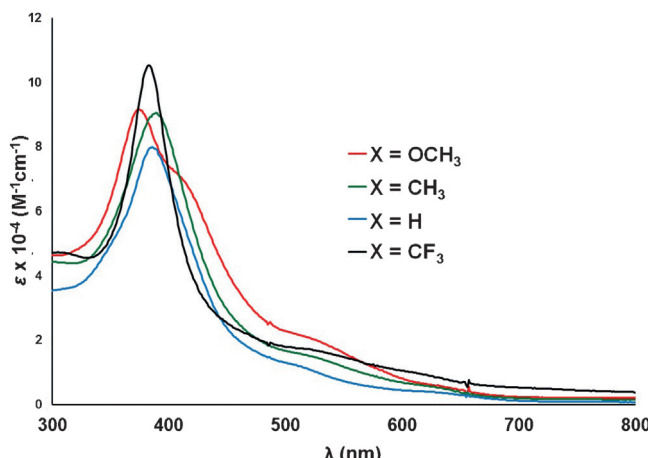


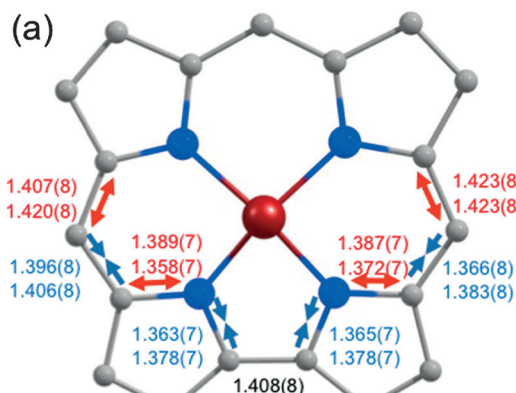
Figure 2. Electronic absorption of $\{Fe[TpXPC]\}_2(\mu\text{-O})$ in dichloromethane.

Table 1. Soret absorption maxima (nm) selected Cu, Fe, and Au [TpXPC] complexes in CH_2Cl_2 .				
Complex	p-Substituent			
	CF_3	H	Me	OMe
$Cu[TpXPC]^a$	407	410	418	434
$Fe[TpXPC]Cl^b$	401	410	419	426
$\{Fe[TpXPC]\}_2(\mu\text{-O})^c$	383	386	389	375, 410
$Au[TpXPC]^d$	419	418	420	420

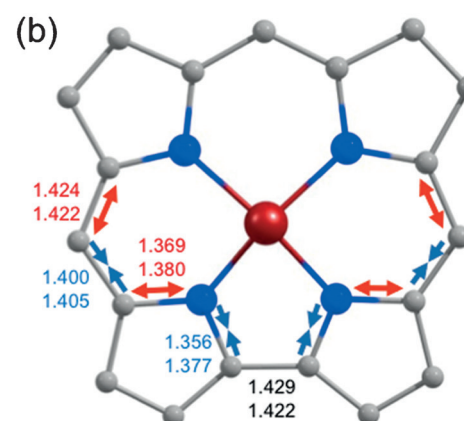
[a] Ref. [10a]. [b] Ref [6]. [c] This work. [d] Ref [16c].

We have recently found that metallocorroles with corrole²⁻ character, including $FeCl$ and $FeNO$ corroles,^[13] exhibit characteristic bond distance alternations in the “southern” part of the corrole macrocycle that includes the bipyrrole unit (Figure 3). No such bond distance alternations are observed for innocent metallocorroles, such $Au^{[16b-d]}$, $OsN^{[17]}$ and $ReO^{[18]}$ corroles. Armed with this perspective, we reexamined the published X-ray crystal structure of $\{Fe[TPFPC]\}_2O^{[10]}$ and found clear evidence of bond length alternations in the “southern” part of the molecule (Figure 3). The suspicion that μ -oxo-diiron corroles might be wolves in sheep’s clothing thus took hold, prompting us to undertake a detailed density functional theoretical (DFT) study of their electronic structure.^[19,20]

The broken-symmetry (BS)^[21,22] $M_S=0$ spin density profile obtained from a B3LYP/ZORA-STO-TZ2P calculation on



$\{Fe[TPFPC]\}_2(\mu\text{-O})$



$\{Fe[TPC]\}_2(\mu\text{-O})$

Figure 3. Bond distance alternations in μ -oxo-diiron corrole structures:
a) The upper and lower values refer to the two symmetry-distinct corrole rings in the crystallographic structure; b) the upper and lower values refer to average B3LYP and BP86 values, both obtained with STO-TZ2P basis sets.

$\{Fe[TPC]\}_2O$ clearly indicated the following intramolecularly spin-coupled description (Figure 1 and Table 2):

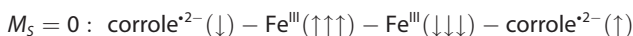


Table 2. Selected B3LYP/STO-TZ2P results for different MS states of $\{Fe[TPC]\}_2O$: relative energies (E_{rel}), Mulliken spin populations ($\rho_{Mulliken}$),^[a] and $\langle S^2 \rangle$ values.

M_S	E_{rel} [eV]	$\rho_{Mulliken}$	TPC	Fe	O	Fe'	TPC'	$\langle S^2 \rangle$
								Calc. (theo.)
0	0.000	-0.758	2.336	0.000	-2.336	0.759	3.159 (0.000)	
1	0.847	-0.665	2.393	0.134	0.569	-0.432	3.802 (2.000)	
2	0.306	-0.599	2.382	0.432	2.382	-0.598	7.144 (6.000)	
3	0.616	0.448	2.373	0.353	2.375	0.450	12.116 (12.000)	
4	1.370	1.076	2.569	0.711	2.569	1.075	20.100 (20.000)	

[a] Negative spin populations are shown in bold.

Importantly, the pure functional BP86 also broke spin symmetry and provided a nearly identical spin-density profile. Furthermore, both B3LYP and BP86 geometry optimizations reproduced the expected bond length alternations (Figure 3).^[7] Finally, in a stringent test of our theoretical method, a vibrational analysis (BS-BP86) of $\{\text{Fe}[\text{TPC}]\}_2\text{O}$ with an STO-TZP basis set reproduced the frequency of the Fe–O–Fe asymmetric stretch (829 cm^{-1}), including the ^{18}O isotope effect (-38 cm^{-1} , Figure 4), with excellent accuracy.^[23]

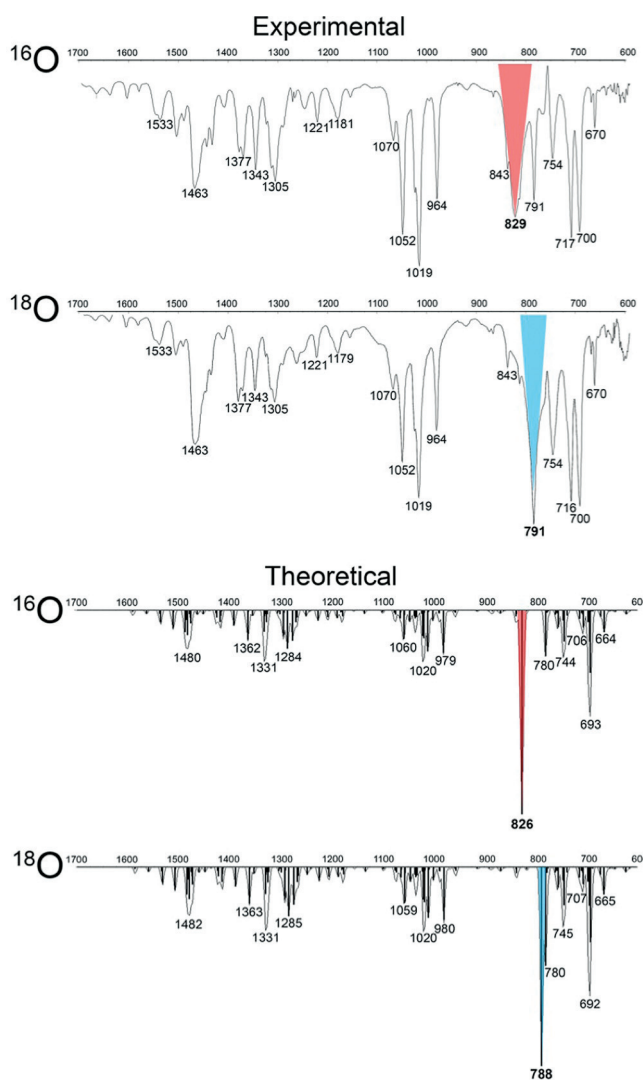


Figure 4. Experimental and simulated (BS-B3LYP/STO-TZP) IR spectra of $\{\text{Fe}[\text{TPC}]\}_2(\mu\text{-O})$, with the Fe–O–Fe asymmetric stretch marked in color.

With the noninnocent electronic–structural description on relatively firm ground, we proceeded to analyze the intramolecular spin couplings in terms of the following Heisenberg–Dirac–van Vleck (HDvV) spin Hamiltonian:

$$H = J_{\text{Fe}-\text{corrole}}(S_{\text{Fe}} \cdot S_{\text{corrole}}) + J_{\text{Fe}-\text{Fe}'}(S_{\text{Fe}} \cdot S_{\text{Fe}'}) + J_{\text{Fe}'-\text{corrole}}(S_{\text{Fe}'} \cdot S_{\text{corrole}}) \quad (1)$$

For that, we needed to evaluate the following $M_S=2$ and $M_S=4$ states, which fortunately turned out to be smoothly convergent:

$$M_S = 2 : \text{corrole}^{2-}(\downarrow) - \text{Fe}^{\text{III}}(\uparrow\uparrow\uparrow) - \text{Fe}^{\text{III}}(\uparrow\uparrow\uparrow) - \text{corrole}^{2-}(\downarrow);$$

$$M_S = 4 : \text{corrole}^{2-}(\uparrow) - \text{Fe}^{\text{III}}(\uparrow\uparrow\uparrow) - \text{Fe}^{\text{III}}(\uparrow\uparrow\uparrow) - \text{corrole}^{2-}(\uparrow).$$

The energies of the three M_S states, given by Equations (2–4),

$$E(M_S = 0) = -\frac{3}{4}J_{\text{Fe}-\text{corrole}} - \frac{9}{4}J_{\text{Fe}-\text{Fe}'} - \frac{3}{4}J_{\text{Fe}'-\text{corrole}'} \quad (2)$$

$$E(M_S = 2) = -\frac{3}{4}J_{\text{Fe}-\text{corrole}} + \frac{9}{4}J_{\text{Fe}-\text{Fe}'} - \frac{3}{4}J_{\text{Fe}'-\text{corrole}'} \quad (3)$$

$$E(M_S = 4) = \frac{3}{4}J_{\text{Fe}-\text{corrole}} + \frac{9}{4}J_{\text{Fe}-\text{Fe}'} + \frac{3}{4}J_{\text{Fe}'-\text{corrole}'} \quad (4)$$

allowed us to evaluate the two unique coupling constants:

$$J_{\text{Fe}-\text{corrole}} = J_{\text{Fe}'-\text{corrole}'} = \frac{1}{3}[E(M_S = 4) - E(M_S = 2)] \quad (5)$$

$$J_{\text{Fe}-\text{Fe}'} = \frac{2}{9}[E(M_S = 2) - E(M_S = 0)] \quad (6)$$

B3LYP/STO-TZ2P calculations yielded the following vertical HDvV coupling constants:

$$J_{\text{Fe}-\text{corrole}} = J_{\text{Fe}'-\text{corrole}'} = 0.355\text{ eV (}2860\text{ cm}^{-1}\text{)}$$

and

$$J_{\text{Fe}-\text{Fe}'} = 0.068\text{ eV (}548\text{ cm}^{-1}\text{)}.$$

The high value of $J_{\text{Fe}-\text{corrole}}$ is qualitatively in accord with that calculated for $\text{Fe}[\text{TPC}]Cl$ (1639 cm^{-1})^[24] and may also be intuitively expected: an electron in an Fe d_{2z} orbital, which is expected to be half-occupied for intermediate-spin Fe^{III} , is ideally situated to strongly couple with a corrole a_{2u} -type radical (permitting ourselves to use porphyrin-type D_{4h} nomenclature for the corrole HOMO). The $J_{\text{Fe}-\text{Fe}'}$ value is also in qualitative accord with that observed for other μ -oxodiiron(III) systems, such as $[\text{Fe}^{\text{III}}_2(\mu\text{-O})(\text{HBpz}_3)_2]^{2+}$ (242 cm^{-1})^[25] and $[\text{Fe}^{\text{III}}_2(\mu\text{-O})(\text{Me}_3\text{TACN})_2]^{4+}$ (238 cm^{-1}).^[26]

In conclusion, μ -oxo-diiron corroles are not true Fe^{IV} complexes but are best viewed as assemblages of four open-shell fragments:

$$\text{corrole}^{2-}(\downarrow) - \text{Fe}^{\text{III}}(\uparrow\uparrow\uparrow) - \text{Fe}^{\text{III}}(\downarrow\downarrow\downarrow) - \text{corrole}^{2-}(\uparrow),$$

with antiferromagnetic coupling between any two adjacent fragments. The clinching evidence has come from DFT calculations, which have done an excellent job of reproducing a) skeletal bond length alternations indicative of a noninnocent corrole and b) the frequency of the Fe–O–Fe asymmetric stretch, including the ^{18}O isotope effect on the latter.^[27] Our revised view of μ -oxo-diiron corroles is clearly of broad relevance. For researchers working on corroles, the present results once again

underscore the ubiquitous nature of noninnocent electronic structures. For the broader bioinorganic chemistry community, a longstanding mystery has been solved: charge delocalization via ligand noninnocence has provided a plausible explanation for the hitherto inexplicable stability of μ -oxo-diiron corroles, relative to other high-valent iron–oxo intermediates.

Experimental Section

Three of the complexes studied, $\{\text{Fe}[\text{TpXPC}]\}_2(\mu\text{-O})$ ($\text{X} = \text{CF}_3$, H, and Me) were synthesized according to previously reported procedures.^[6] The $\text{X}=\text{OMe}$ complex is a new compound and was synthesized stepwise as described below.

Fe[TpOMePC]Cl: Anhydrous FeCl_2 (165 mg, 1.3 mmol, 20 equiv) was added to a DMF (20 mL) solution of $\text{H}_3[\text{TpOMePC}]$ (40 mg, 0.065 mmol) in a 100 mL two-necked round-bottomed flask. Argon was bubbled through the solution for 5 min. The reaction mixture was then heated to reflux (165 °C) under argon and progress of the reaction was monitored with UV/Vis spectroscopy and mass spectrometry. After 20–30 min, heating was discontinued and the red–brown solution, after cooling to near room temperature, was rotary-evaporated to dryness. The dark-brown residue was chromatographed on a short silica gel (Davisil, 35–70 μm particle size, 150 Å pore size) column with 1:1 dichloromethane/diethyl ether as eluent. The Fe^{III} –ether complex was collected, dried, and re-dissolved in 10 mL dichloromethane. The dichloromethane solution was then shaken with 7% HCl solution (15 mL \times 3), washed twice with distilled water, dried over anhydrous Na_2SO_4 , filtered, and the solvent was rotary evaporated. The red–brown residue was chromatographed over a short neutral alumina column with chloroform as eluent to afford $\text{Fe}[\text{TpOMePC}]Cl$ (31 mg, 0.044 mmol) in 68% yield. UV/Vis (CH_2Cl_2): λ_{max} (nm), [$\varepsilon \times 10^{-4}, (\text{M}^{-1}\text{cm}^{-1})$]: 379 [3.17], 426 [2.26]. ^1H NMR (CDCl_3): δ 26.5 (s, 2 H, aryl-ortho), 25.2 (s, 2 H, aryl-ortho), 24.5 (s, 2 H, aryl-ortho), 5.56 (br s, 2 H, β -pyrrolic), 2.1 (s, 3 H, 10-p-MeO), 1.9 (s, 6 H, 5,15-p-MeO), –2.3 (s, 4 H, aryl-meta), –3.48 (s, 1 H, aryl-meta), –3.77 (s, 1 H, aryl-meta), –4.55 (s, 2 H, β -pyrrolic), –7.28 (s, 2 H, β -pyrrolic), –41.1 (br s, 2 H, β -pyrrolic). HRMS (ESI $^-$, major isotopomer): $[\text{M}]^- = 704.1286$ (expt), 704.1284 (calc).

$\{\text{TpOMePC}\text{Fe}\}_2\text{O}$: A solution of $\text{Fe}[\text{TpOMePC}]Cl$ (20 mg, 0.0284 mmol) in dichloromethane (5 mL) was vigorously stirred with 2 M aqueous NaOH (15 mL) for 1 h at room temperature.^[28] The organic phase was then shaken twice with 2 M aqueous NaOH (15 mL \times 2, to ensure complete reaction), dried with anhydrous Na_2SO_4 , filtered, and rotary-evaporated to dryness. The dark brown residue was purified by column chromatography on neutral alumina (activated, Brockman I) with chloroform as eluent to afford the pure product (17.5 mg, 0.0129 mmol) in 92% yield. UV/Vis (CH_2Cl_2): λ_{max} (nm), [$\varepsilon \times 10^{-4}, (\text{M}^{-1}\text{cm}^{-1})$]: 375 (9.17), 410 (sh) (7.06). ^1H NMR (CD_2Cl_2 , –15 °C): δ 7.56 (d, $J = 7.56$ Hz, 4 H, β -pyrrolic), 7.41 (d, $J = 8.52$ Hz, 4 H, β -pyrrolic), 7.38–7.34 (m, 10 H, meso-aryl), 7.09 (d, $J = 4.56$ Hz, 4 H, β -pyrrolic), 7.03–6.98 (m, 6 H, overlapping β -pyrrolic and/or meso-aryl), 6.90–6.94 (m, 10 H, overlapping β -pyrrolic and/or meso-aryl), 6.81 (d, $J = 8.4$ Hz, 2 H, meso-aryl), 3.92 (s, 12 H, 5,15-pOMe protons), 3.87 (s, 6 H, 10-pOMe protons). HRMS (ESI $^+$, major isotopomer): $[\text{M}]^+ = 1354.3124$ (expt), 1354.3128 (calc).

Acknowledgements

This work was supported by FRINATEK project 231086 of the Research Council of Norway (AG).

Keywords: corroles • density functional calculations • iron • spin coupling • structure elucidation

- [1] For a Review, see: J. Hohenberger, K. Ray, K. Meyer, *Nat. Commun.* **2012**, 3, 720.
- [2] For a Minireview, see: C. M. Krest, E. L. Onderko, T. H. Yosca, J. C. Calixto, R. F. Karp, J. Livada, J. Rittle, M. T. Green, *J. Biol. Chem.* **2013**, 288, 17074–17081.
- [3] a) R. Banerjee, Y. Proshlyakov, J. D. Lipscomb, D. A. Proshlyakov, *Nature* **2015**, 518, 431–434.
- [4] For a Review, see: L. Que, Jr., *Acc. Chem. Res.* **2007**, 40, 493–500.
- [5] E. Vogel, S. Will, A. S. Tillig, L. Neumann, J. Lex, E. Bill, A. X. Trautwein, K. Wieghardt, *Angew. Chem. Int. Ed. Engl.* **1994**, 33, 731–735; *Angew. Chem.* **1994**, 106, 771–775.
- [6] E. Steene, T. Wondimagegn, A. Ghosh, *J. Phys. Chem. B* **2001**, 105, 11406–11413; addition/correction: E. Steene, T. Wondimagegn, A. Ghosh, *J. Phys. Chem. B* **2002**, 106, 5312–5312.
- [7] L. Simkhovich, A. Mohammed, I. Goldberg, Z. Gross, *Chem. Eur. J.* **2001**, 7, 1041–1055.
- [8] For reviews on metallocorroles, see: a) I. Aviv-Harel, Z. Gross, *Coord. Chem. Rev.* **2011**, 255, 717–736; b) K. E. Thomas, A. Alemanyehu, J. Conradie, C. M. Beavers, A. Ghosh, *Acc. Chem. Res.* **2012**, 45, 1203–1214; c) J. H. Palmer, *Struct. Bonding (Berlin)* **2011**, 142, 49–90; d) H. L. Buckley, J. Arnold, *Dalton Trans.* **2015**, 44, 30–36.
- [9] Copper corroles are inherently saddled, as a result of ligand noninnocence; see: a) A. B. Alemanyehu, E. Gonzalez, L.-K. Hansen, A. Ghosh, *Inorg. Chem.* **2009**, 48, 7794–7799; b) M. Bröring, F. Brégier, E. C. Tejero, C. Hell, M. C. Holthausen, *Angew. Chem. Int. Ed.* **2007**, 46, 445–448; *Angew. Chem.* **2007**, 119, 449–452.
- [10] For other early work on copper corroles, see: a) I. H. Wasbotten, T. Wondimagegn, A. Ghosh, *J. Am. Chem. Soc.* **2002**, 124, 8104–8116; b) C. Brückner, R. P. Briñas, J. A. K. Bauer, *Inorg. Chem.* **2003**, 42, 4495–4497; c) A. Alemanyehu, J. Conradie, A. Ghosh, *Eur. J. Inorg. Chem.* **2011**, 1857–1864..
- [11] For strongly saddled Cu corroles, see: a) K. E. Thomas, I. H. Wasbotten, A. Ghosh, *Inorg. Chem.* **2008**, 47, 10469–10478; b) A. B. Alemanyehu, L.-K. Hansen, A. Ghosh, *Inorg. Chem.* **2010**, 49, 7608–7610; c) K. E. Thomas, J. Conradie, L.-K. Hansen, A. Ghosh, *Eur. J. Inorg. Chem.* **2011**, 1865–1870; d) S. Berg, K. E. Thomas, C. M. Beavers, A. Ghosh, *Inorg. Chem.* **2012**, 51, 9911–9916.
- [12] a) O. Zakharieva, V. Schünemann, M. Gerdan, S. Licoccia, S. Cai, F. A. Walker, A. X. Trautwein, *J. Am. Chem. Soc.* **2002**, 124, 6636–6648; b) For a review, see: F. A. Walker, S. Licoccia, R. Paolesse, *J. Inorg. Biochem.* **2006**, 100, 810–837; c) B. O. Roos, V. Veryazov, J. Conradie, P. R. Taylor, A. Ghosh, *J. Phys. Chem. A J. Phys. Chem. B* **2008**, 112, 14099–14102; d) R. K. Hocking, S. D. George, Z. Gross, F. A. Walker, K. O. Hodgson, B. Hedman, E. I. Solomon, *Inorg. Chem.* **2009**, 48, 1678–1688.
- [13] a) H. Vazquez-Lima, H.-K. Norheim, A. Ghosh, *Dalton Trans.* **2015**, 44, 10146–10151; b) H.-K. Norheim, J. Capar, R. F. Einrem, K. J. Gagnon, C. M. Beavers, H. Vazquez-Lima, A. Ghosh, *Dalton Trans.* **2016**, 45, 681–689.
- [14] A. Ghosh, E. Steene, *J. Inorg. Biochem.* **2002**, 91, 423–436.
- [15] A. B. Alemanyehu, H. Vazquez-Lima, C. M. Beavers, K. J. Gagnon, J. Bendix, A. Ghosh, *Chem. Commun.* **2014**, 50, 11093–11096.
- [16] a) A. B. Alemanyehu, A. Ghosh, *J. Porphyrins Phthalocyanines* **2011**, 15, 106–110; b) E. Rabinovich, I. Goldberg, Z. Gross, *Chem. Eur. J.* **2011**, 17, 12294–12301; c) K. E. Thomas, A. B. Alemanyehu, J. Conradie, C. M. Beavers, A. Ghosh, *Inorg. Chem.* **2011**, 50, 12844–12851; d) K. E. Thomas, C. M. Beavers, A. Ghosh, *Mol. Phys.* **2012**, 110, 2439–2444.
- [17] A. B. Alemanyehu, K. J. Gagnon, J. Terner, A. Ghosh, *Angew. Chem. Int. Ed.* **2014**, 53, 14411–14414; *Angew. Chem.* **2014**, 126, 14639–14642.
- [18] R. F. Einrem, K. J. Gagnon, A. B. Alemanyehu, A. Ghosh, *Chem. Eur. J.* **2016**, 22, 517–520.
- [19] For an early review of DFT calculations on noninnocent porphyrin-type complexes, see: A. Ghosh, E. Steene, *J. Biol. Inorg. Chem.* **2001**, 6, 739–752.
- [20] For a review of DFT calculations on Fe-containing bioinorganic systems, see: H. Hirao, N. Thellamurege, X. Zhang, *Front. Chem.* **2014**, 2, 14.
- [21] L. Noddeman, *J. Chem. Phys.* **1981**, 74, 5737–5743.

- [22] L. Noddleman, D. Post, E. J. Baerends, *Chem. Phys.* **1982**, *64*, 159–166.
- [23] The Fe–O–Fe asymmetric stretch [cm^{-1}] for the other $\{\text{Fe}[\text{TpXPC}]\}_2\text{O}$ derivatives have been assigned as ($^{16}\text{O}/^{18}\text{O}$): CF_3 (821/792), Me (832/795), and MeO (820/790).
- [24] Spin coupling in $\text{Fe}[\text{TPC}]\text{Cl}$ involves an intermediate-spin ($S=3/2$) Fe^{II} center and a corrole $^{2-}$ radical, which leads to: $J_{\text{Fe-corrole}} = \frac{2}{3}[E(M_S = 2) - E(M_S = 1)]$.
- [25] W. H. Armstrong, A. Spool, G. C. Papaefthymiou, R. B. Frankel, S. J. Lippard, *J. Am. Chem. Soc.* **1984**, *106*, 3653–3667.
- [26] J. A. R. Hartman, R. L. Rardin, P. Chaudhuri, K. Pohl, K. Wieghardt, B. Nuber, J. Weiss, G. C. Papaefthymiou, R. B. Frankel, S. J. Lippard, *J. Am. Chem. Soc.* **1987**, *109*, 7387–7396.
- [27] A detailed Mössbauer spectroscopic study of the compounds reported herein is in progress and will be reported in due course.
- [28] The ^{18}O -labeled μ -oxo-diiron corroles were synthesized using $2\text{ M Na}^{18}\text{OH}$ in H_2^{18}O , which was prepared as described in: T. Kurahashi, *Inorg. Chem.* **2015**, *54*, 8356–8366.

Received: March 6, 2016

Published online on June 22, 2016

Supporting Information

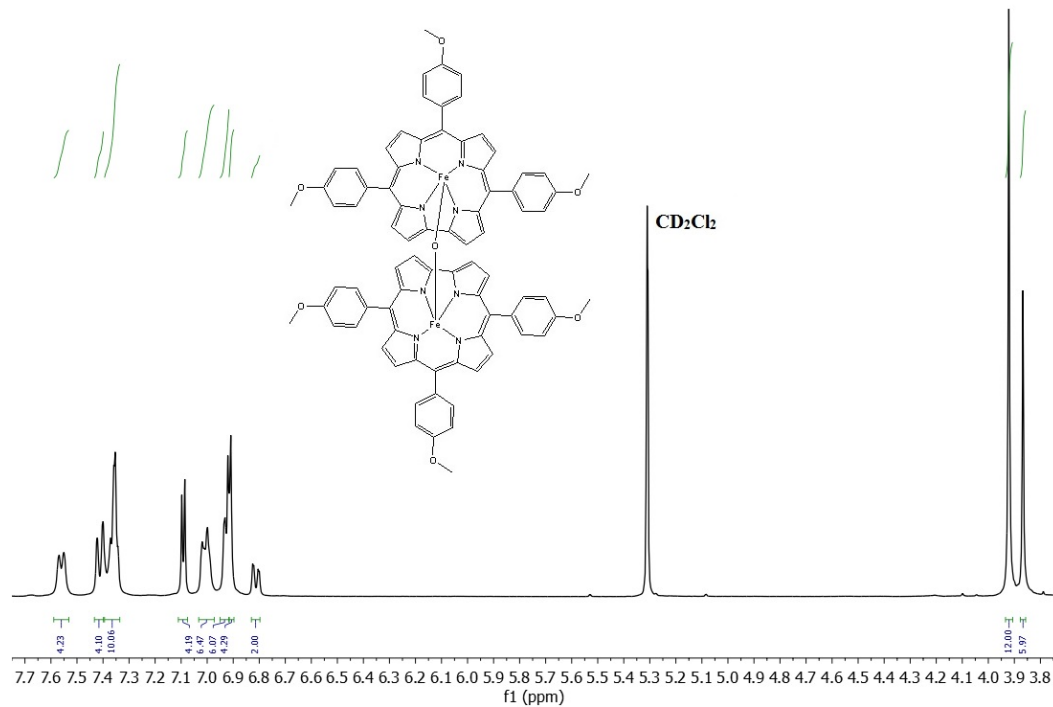
Wolves in Sheep's Clothing: μ -Oxo Diiron Corroles Revisited

Sumit Ganguly,^[a] Hugo Vazquez-Lima,*^[a] and Abhik Ghosh*^[a]

[a] *Sumit Ganguly, Dr. Hugo Vazquez-Lima,* and Professor Dr. Abhik Ghosh**
Department of Chemistry
UiT – The Arctic University of Norway
9037 Tromsø, Norway
E-mail: hugo.vazquez@uit.no (HVL), abhik.ghosh@uit.no (AG)

A. Spectra for [(TpOMePC)Fe]₂O

(a)



(b)

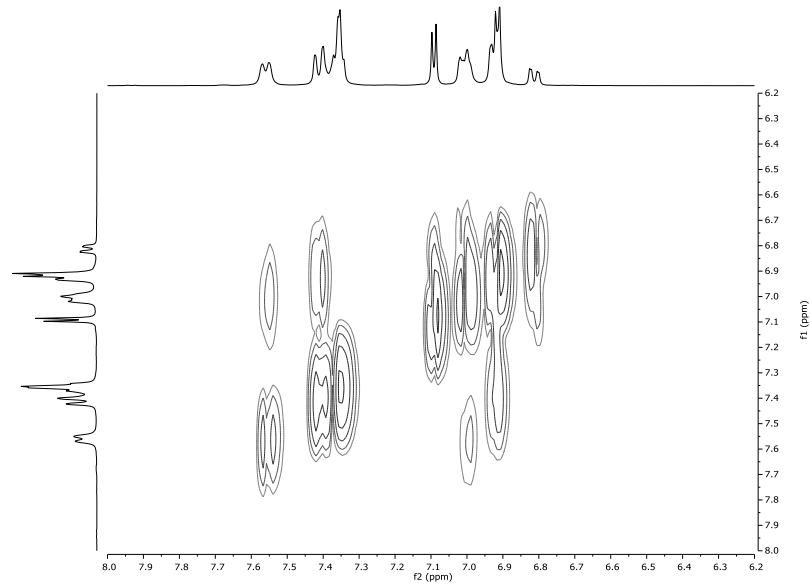


Figure S1. ¹H NMR spectra of [(TpOMePC)Fe]₂O in CD₂Cl₂ at -15°C: (a) 1D spectrum and (b) ¹H-¹H COSY.

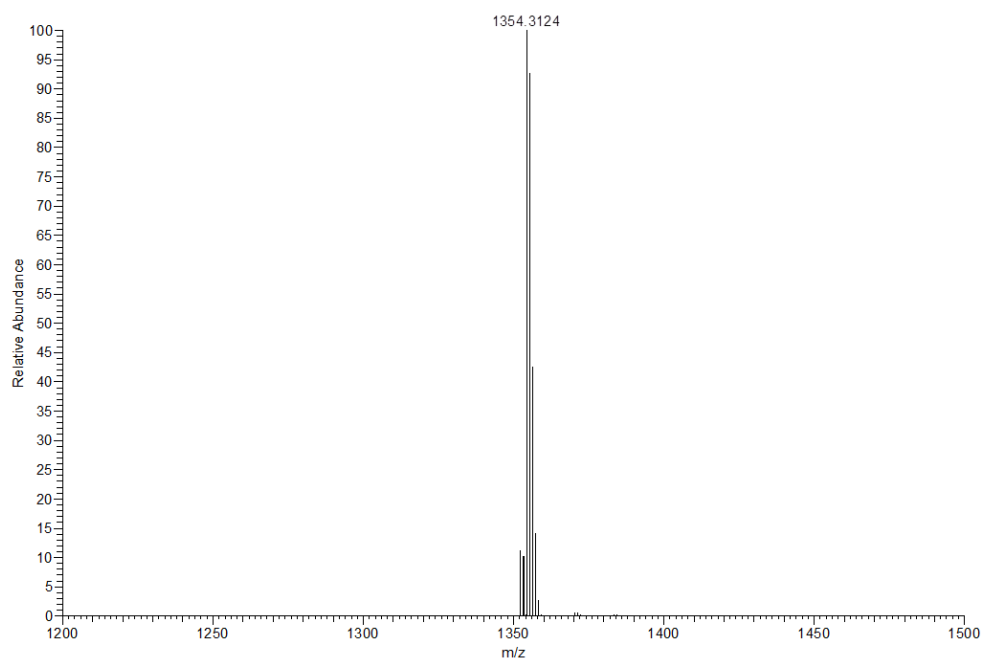


Figure S2. Positive-mode ESI mass spectrum for $[(TpOCH_3PC)Fe]_2O$.

Computational methods. In general, the calculations were carried out with the ADF^[1] 2014 program system using the B3LYP^[2] and BP86^[2a,3] exchange-correlation functionals. Scalar relativistic effects were taken into account with the ZORA Hamiltonian^[4] and all-electron ZORA STO-TZ2P^[5] basis sets and dispersion effects were accounted for with Grimme's D3 correction.^[6] The only exceptions to these general methods were the vibrational analyses, where we employed a ZORA STO-TZP basis set. The optimized geometries were confirmed as minima by the absence of imaginary frequencies.

- [1] (a) G. te Velde, F. M. Bickelhaupt, E. J. Baerends, C. Fonseca Guerra, S. J. A. van Gisbergen, J. G. Snijders, T. Ziegler, *J. Comput. Chem.* **2001**, *22*, 931-967. (b) C. Fonseca Guerra, J. G. Snijders, G. te Velde, E. J. Baerends, *Theor. Chem. Acc.* **1998**, *99*, 391-403.
- [2] (a) A. D. Becke, *Phys. Rev. A* **1988**, *38*, 3098-3100. (b) C. Lee, W. Yang, R. G. Parr, *Phys. Rev. B* **1988**, *37*, 785-789. (c) T. V. Russo, R. L. Martin, P. J. Hay, *J. Chem. Phys.* **1994**, *101*, 7729-7737. (d) B. G. Johnson, P. M. W. Gill, J. A. Pople, *J. Chem. Phys.* **1993**, *98*, 5612-5626. (e) P. J. Stephens, F. J. Devlin, C. F. Chabalowski, M. J. Frisch, *J. Phys. Chem.* **1994**, *98*, 11623-11627.
- [3] J. P. Perdew, J. A. Chevary, S. H. Vosko, K. A. Jackson, M. R. Pederson, D. J. Singh, C. Fiolhais, *Phys. Rev. B* **1992**, *46*, 6671-6687.
- [4] (a) E. van Lenthe, A. Ehlers, E.-J. Baerends, *J. Chem. Phys.* **1999**, *110*, 8943-8953. (b) E. van Lenthe, E. J. Baerends, J. G. Snijders, *J. Chem. Phys.* **1993**, *99*, 4597-4610. (c) E. van Lenthe, E. J. Baerends, J. G. Snijders, *J. Chem. Phys.* **1994**, *101*, 9783-9792. (d) E. van Lenthe, J. G. Snijders, E. J. Baerends, *J. Chem. Phys.* **1996**, *105*, 6505-6516. (e) E. van Lenthe, R. van Leeuwen, E. J. Baerends, J. G. Snijders, *Int. J. Quantum Chem.* **1996**, *57*, 281-293.
- [5] E. Van Lenthe, E. J. Baerends, *J. Comput. Chem.* **2003**, *24*, 1142-1156.
- [6] S. Grimme, J. Antony, S. Ehrlich, H. Krieg, *J. Chem. Phys.* **2010**, *132*, 154104.

**C. Symmetry-unconstrained optimized Cartesian coordinates (\AA) for
 $\{\text{Fe[TPC]}\}_2(\mu\text{-O})$**

1. Broken-symmetry ($M_s = 0$) B3LYP-D3/STO-TZ2P

Fe	-1.865527	-1.669510	-0.441414
Fe	1.396289	-2.912640	-0.419503
O	-0.284858	-2.424078	-0.482044
N	-1.508538	0.160575	-0.859923
N	-2.455005	-1.921731	-2.280826
N	-2.912422	-3.165627	0.226547
N	-1.973258	-0.879183	1.302330
N	2.102795	-1.928342	1.057751
N	1.305043	-4.481322	0.723257
N	1.476216	-3.960532	-2.056385
N	2.320304	-1.501392	-1.338581
C	-1.226609	0.993188	0.173106
C	-0.799428	2.243894	-0.355808
C	-0.841682	2.133405	-1.730037
C	-1.294416	0.807011	-2.047621
C	-1.588991	0.193644	-3.269908
C	-2.153761	-1.111567	-3.352485
C	-2.482216	-1.822640	-4.554650
C	-2.974964	-3.045115	-4.196337
C	-2.941614	-3.115076	-2.766514
C	-3.339643	-4.205032	-1.965699
C	-3.352831	-4.208167	-0.554575
C	-3.767230	-5.275505	0.306475
C	-3.567700	-4.863155	1.593955
C	-3.011701	-3.543282	1.546370
C	-2.643665	-2.745556	2.666662
C	-2.167963	-1.435868	2.538587
C	-1.776865	-0.452832	3.510010
C	-1.357959	0.669955	2.825443
C	-1.479446	0.377030	1.437971
C	2.592880	-0.689276	0.806782
C	2.871771	-0.049894	2.047116
C	2.547146	-0.948425	3.041637
C	2.057006	-2.142003	2.408984
C	1.665948	-3.380541	2.928768
C	1.324641	-4.487705	2.100475
C	0.904362	-5.784707	2.546218
C	0.633240	-6.538485	1.439434
C	0.870839	-5.714103	0.292368
C	0.711451	-6.080507	-1.060286
C	1.033386	-5.258884	-2.162246
C	0.919483	-5.585665	-3.553489

C	1.288234	-4.479203	-4.264749
C	1.620627	-3.448464	-3.327180
C	2.048514	-2.128673	-3.647336
C	2.412697	-1.195063	-2.670197
C	2.889882	0.156613	-2.759128
C	3.073872	0.622486	-1.472912
C	2.699751	-0.432179	-0.594599
C	-1.290412	0.932799	-4.522323
C	-2.277414	1.186659	-5.481332
C	0.008123	1.397262	-4.756837
C	-1.967992	1.880102	-6.644076
C	0.316722	2.086677	-5.922578
C	-0.669570	2.328419	-6.871821
C	-3.736382	-5.457106	-2.666099
C	-2.799951	-6.136142	-3.450034
C	-5.025731	-5.983861	-2.548584
C	-3.139168	-7.318423	-4.093744
C	-5.366506	-7.164293	-3.200341
C	-4.423090	-7.836810	-3.971315
C	-2.736885	-3.341954	4.023311
C	-1.998191	-4.487009	4.335784
C	-3.513984	-2.749070	5.023027
C	-2.027248	-5.021530	5.616319
C	-3.546929	-3.287840	6.304055
C	-2.802473	-4.423667	6.604330
C	1.596298	-3.527685	4.403792
C	0.772348	-2.674316	5.144756
C	2.341857	-4.498906	5.080024
C	0.680122	-2.800117	6.524038
C	2.255947	-4.616345	6.461566
C	1.420798	-3.772175	7.188269
C	0.128406	-7.421609	-1.340909
C	0.839360	-8.395419	-2.046913
C	-1.165465	-7.716559	-0.904373
C	0.266286	-9.633414	-2.315394
C	-1.741900	-8.949173	-1.181350
C	-1.029145	-9.910679	-1.888610
C	2.077764	-1.706896	-5.070773
C	3.247230	-1.214349	-5.658196
C	0.911969	-1.763790	-5.841419
C	3.248695	-0.790909	-6.982694
C	0.912770	-1.336151	-7.162275
C	2.081103	-0.847272	-7.738740
H	-0.513483	3.110862	0.217069
H	-0.604359	2.899671	-2.448159
H	-2.371389	-1.443349	-5.556183
H	-3.324771	-3.824768	-4.851529

H	-4.170068	-6.219458	-0.015733
H	-3.788973	-5.409389	2.493965
H	-1.817136	-0.578274	4.578007
H	-0.998454	1.593055	3.250321
H	3.279017	0.939177	2.176631
H	2.653546	-0.807421	4.104411
H	0.824195	-6.094988	3.573336
H	0.300999	-7.561870	1.414409
H	0.604780	-6.535716	-3.948692
H	1.338740	-4.386567	-5.335678
H	3.078265	0.695219	-3.671701
H	3.426314	1.599394	-1.184559
H	-3.290087	0.849244	-5.303752
H	0.776136	1.191297	-4.025526
H	-2.744136	2.075425	-7.373292
H	1.332824	2.418261	-6.095348
H	-0.430371	2.862231	-7.783596
H	-1.796222	-5.741259	-3.527404
H	-5.763201	-5.456787	-1.957197
H	-2.390837	-7.844758	-4.672556
H	-6.373602	-7.553261	-3.112505
H	-4.686867	-8.757098	-4.475270
H	-1.375255	-4.932823	3.573850
H	-4.100865	-1.871894	4.786138
H	-1.422068	-5.888086	5.849930
H	-4.159954	-2.823805	7.066026
H	-2.823176	-4.836890	7.604629
H	0.181352	-1.936945	4.619009
H	2.998558	-5.152409	4.520739
H	0.014078	-2.149822	7.077501
H	2.849077	-5.365383	6.973473
H	1.348774	-3.872581	8.263409
H	1.849716	-8.183581	-2.372593
H	-1.725442	-6.964556	-0.365284
H	0.832769	-10.380541	-2.856724
H	-2.756218	-9.149946	-0.862847
H	-1.481839	-10.868516	-2.111276
H	4.158944	-1.182957	-5.074357
H	0.001326	-2.124464	-5.386050
H	4.165635	-0.425716	-7.426815
H	-0.007105	-1.364994	-7.733726
H	2.081198	-0.509310	-8.767689

2. Broken-symmetry ($M_s = 0$) BP86-D3/STO-TZ2P for {Fe[TPC]}₂(μ-O)

Fe	1.359548	-2.891491	-0.420433
Fe	-1.799840	-1.685790	-0.442821
O	-0.245698	-2.355475	-0.456954
N	1.225978	-4.455249	0.708756
N	1.416655	-3.923725	-2.058246
N	2.079983	-1.932039	1.059478
N	2.301549	-1.489810	-1.324277
N	-1.462756	0.139251	-0.876809
N	-1.909323	-0.878041	1.289186
N	-2.375743	-1.967276	-2.268076
N	-2.821268	-3.181919	0.240399
C	0.004546	-7.382178	-1.372692
C	0.047066	-9.582989	-2.402565
C	0.132087	1.320881	-4.760869
C	0.473903	-2.707530	6.495862
C	0.481980	1.975436	-5.939235
C	0.520664	-6.521468	1.413003
C	0.619259	-6.057616	-1.087524
C	0.638893	-2.594665	5.117675
C	0.669373	-8.365165	-2.122694
C	0.774756	-5.695049	0.268971
C	0.785872	-1.285991	-7.143521
C	0.788509	-5.771585	2.531345
C	0.827870	-1.740631	-5.828291
C	0.859250	-5.547829	-3.577892
C	0.958709	-5.231987	-2.181038
C	1.113093	-3.732732	7.196269
C	1.223602	-4.471505	2.103272
C	1.243382	-4.434455	-4.283710
C	1.438486	-3.508954	4.410878
C	1.566547	-3.373850	2.939228
C	1.570186	-3.403403	-3.339903
C	1.924910	-4.638201	6.508128
C	1.928347	-0.740601	-7.733047
C	1.999755	-2.141790	2.420089
C	2.009323	-2.086412	-3.654338
C	2.009792	-1.653007	-5.072703
C	2.089131	-4.527410	5.126903
C	2.398597	-1.168944	-2.664149
C	2.488608	-0.954472	3.065399
C	2.589161	-0.673692	0.823816
C	2.706302	-0.411913	-0.568841
C	2.848476	-0.050123	2.076687
C	2.904074	0.174996	-2.743366
C	3.096333	0.636539	-1.449335

C	3.113297	-0.659077	-6.997619
C	3.155663	-1.110462	-5.677658
C	-0.474711	2.186274	-6.934638
C	-0.731061	2.237392	-0.397639
C	-0.765527	2.100869	-1.777811
C	-1.172475	1.002525	0.156248
C	-1.179132	0.858047	-4.556008
C	-1.225460	0.773074	-2.078159
C	-1.245930	-9.836496	-1.936714
C	-1.289754	-7.654223	-0.898736
C	-1.317126	0.707754	2.807004
C	-1.423697	0.403886	1.420658
C	-1.510449	0.141274	-3.300389
C	-1.731727	-0.417561	3.503984
C	-1.786048	1.746114	-6.736659
C	-1.910784	-8.868552	-1.180862
C	-1.950044	-4.515597	4.343850
C	-1.958512	-5.050812	5.629086
C	-2.081590	-1.158878	-3.366029
C	-2.103011	-1.422053	2.543732
C	-2.137514	1.089743	-5.556773
C	-2.431589	-1.881763	-4.556673
C	-2.562415	-2.741290	2.693001
C	-2.636953	-3.323749	4.054784
C	-2.659324	-4.407161	6.651548
C	-2.682493	-6.161883	-3.459355
C	-2.865131	-3.176041	-2.751290
C	-2.916091	-3.110369	-4.182596
C	-2.922979	-3.550640	1.578763
C	-2.983363	-7.363498	-4.096043
C	-3.256551	-4.265628	-1.942183
C	-3.269979	-4.249335	-0.531037
C	-3.345543	-2.688822	5.088451
C	-3.355031	-3.227665	6.375702
C	-3.492146	-4.867229	1.638337
C	-3.628162	-5.528703	-2.635347
C	-3.693831	-5.299705	0.350914
C	-4.238617	-7.951606	-3.925649
C	-4.890361	-6.122508	-2.477273
C	-5.191672	-7.325725	-3.117792
H	0.122592	-1.815105	4.560138
H	0.185284	-7.551669	1.376723
H	0.547430	-6.503750	-3.982728
H	0.577529	-10.339322	-2.981889
H	0.706554	-6.090405	3.564144
H	0.878924	1.126555	-3.992970
H	0.978963	-3.827519	8.274091

H	1.312040	-4.333918	-5.361035
H	1.511626	2.299270	-6.090935
H	1.682400	-8.171982	-2.475849
H	1.895277	-0.377688	-8.760517
H	2.440596	-5.431358	7.050384
H	2.575763	-0.818986	4.138034
H	2.737830	-5.223178	4.594870
H	3.111004	0.713934	-3.661466
H	3.271496	0.938975	2.220166
H	3.475779	1.609342	-1.153808
H	4.013240	-0.247999	-7.456087
H	4.084936	-1.060888	-5.110072
H	-0.067538	-2.139867	-5.354758
H	-0.149265	-1.334256	-7.701713
H	-0.176303	-2.007278	7.020105
H	-0.200810	2.690929	-7.861355
H	-0.447472	3.122144	0.163390
H	-0.519662	2.856972	-2.515559
H	-0.978305	1.648176	3.229259
H	-1.380348	-4.996871	3.550489
H	-1.395372	-5.960376	5.838941
H	-1.697392	-5.710343	-3.570101
H	-1.733243	-10.784806	-2.164201
H	-1.786546	-0.528531	4.581312
H	-1.812210	-6.886165	-0.329829
H	-2.225887	-7.853703	-4.707763
H	-2.334642	-1.500967	-5.566826
H	-2.543035	1.921911	-7.501528
H	-2.660949	-4.820756	7.660151
H	-2.927190	-9.048387	-0.830487
H	-3.165706	0.765614	-5.396280
H	-3.281937	-3.898138	-4.831006
H	-3.730517	-5.399426	2.552296
H	-3.902880	-1.777722	4.870572
H	-3.915737	-2.726844	7.165606
H	-4.109770	-6.250391	0.037676
H	-4.473787	-8.895244	-4.418370
H	-5.638480	-5.628064	-1.857425
H	-6.178287	-7.772231	-2.990272